Field-Directed Self-Assembly of Magnetic Nanoparticles

Y. Sahoo,[†,‡] M. Cheon,[‡,§] S. Wang,[‡,§] H. Luo,[‡,§] E. P. Furlani,[‡] and P. N. Prasad*[,†,‡,§]

Department of Chemistry, Department of Physics, and Institute for Lasers, Photonics and Biophotonics, University at Buffalo, State University of New York, Buffalo, New York 14260

Received: October 9, 2003

Fe_3O_4 nanoparticles in the size range of 8−12 nm have been prepared and allowed to self-assemble on GaAs substrates in the presence of strong magnetic fields. A long range ordering is observed in which the particles self-assemble into a distribution of elongated clusters with a predominant orientation lengthwise along the field direction. Hysteresis loops measured parallel and perpendicular to the alignment direction show substantial directional dependence. The coercive fields in the direction parallel to the alignment field are larger than those perpendicular to it by 57% and 136% at 100 and 5K, respectively. A broad peak is observed in magnetization profiles obtained with zero- field-cooling.

Nanostructured materials have attracted a great deal of attention for a wide range of reasons. Some of their properties are different from, and in some cases superior to, that of their bulk counterparts. Among the enhanced properties of nanostructured materials, magnetic particles offer a good example with important technological implications. They are ideal for studying such phenomena such as superparamagnetism,[1] magnetization quantum tunneling,[2] magneto-electrical transport, etc.[3,4] They also have immense potential for applications in the areas of high-density data storage,[5] ferrofluids,[6] magnetic resonance imaging (as contrast agents), color processing, and magnetic refrigeration.[7] For many applications such as those involving electrical transport and magnetic switching, the ordering of nanoparticles has a critical role. In this Letter, we present a study on the magnetic field-directed self-assembly of magnetite nanoparticles, and the directional dependence of their collective magnetization. There have been a large number of studies focusing on magnetic anisotropy related to sample geometries, which can be utilized for device purposes.[8−10] Such samples are typically fabricated with lithographic techniques. The field-directed assembly of magnetic particles will provide an inexpensive technique for realizing the same effects.

An assembly of single domain particles makes an ideal system for investigating interparticle effects and their impact on the temperature-dependent magnetization process. Of particular interest is the effect of magnetic interactions on the relaxation time of the magnetic moments of the nanoparticles. Presently, various theories exist for analyzing temperature-dependent interparticle interactions and their effect on the magnetization of nanoparticle systems.[11−19] These theories typically start with a specification (explicit or statistical) of the geometric ordering of the nanoparticles. On the other hand, relatively few results exist for predicting the long-range geometrical ordering of self-assembled particles. In this article, new data are presented on the long-range order and self-assembly of Fe_3O_4 nanoparticles under the influence of strong applied fields. The degree of self-assembly is observed to be field dependent, with finer structures obtained at higher fields. Temperature-dependent magnetization data are presented for the system with the highest degree of self-assembled order, which was obtained at the highest alignment field strength.

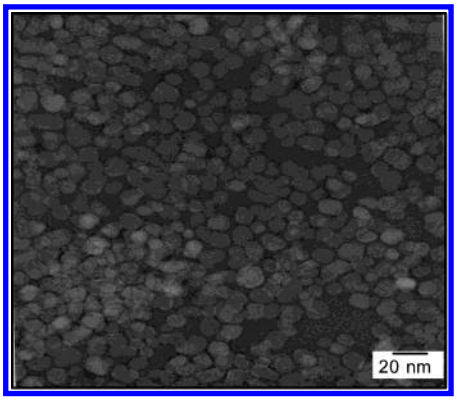

Figure 1. Transmission electron micrograph of Fe_3O_4 nanoparticles.

In the present work, Fe_3O_4 nanoparticles were prepared by an established procedure of precipitating Fe^{2+} and Fe^{3+} in a basic solution.[20] Briefly, a mixture of aqueous solutions of $FeCl_2$ and $FeCl_3$ (1:2 molar ratio) was reacted with three molar equiv of NH_4OH at 80 °C in an anaerobic atmosphere. The resulting black mass was a precipitate of Fe_3O_4 particles, which were subsequently coated with oleic acid. The coated particles were dispersed in a nonpolar solvent: hexane or heptane. They formed a stable dispersion that retained its stability without agglomerating. Size selective precipitation was carried out by adding a nonsolubilizing solvent such as acetone to the dispersion and centrifuging the mixture at different speeds. The fractions obtained were redispersed in heptane. In our samples, the sizes ranged from 8 to 12 nm, as shown in the transmission electron micrograph (Figure 1). The dispersion was drop-cast on a GaAs wafer of size 4 × 3 mm^2 and dried under ambient conditions in the presence of an applied magnetic field which influenced the self-assembly.

The experimental results demonstrate that applied fields are effective in ordering the magnetic nanoparticles. Fields of magnitudes 0.8, 6, 11, and 17 T were available, and it was found that the degree of self-assembly increased with higher fields. The topography of the assembled particles was examined using

[†] Department of Chemistry.
[‡] Institute for Lasers, Photonics and Biophotonics.
[§] Department of Physics.

10.1021/jp031148i CCC: $27.50
Published on Web 02/20/2004

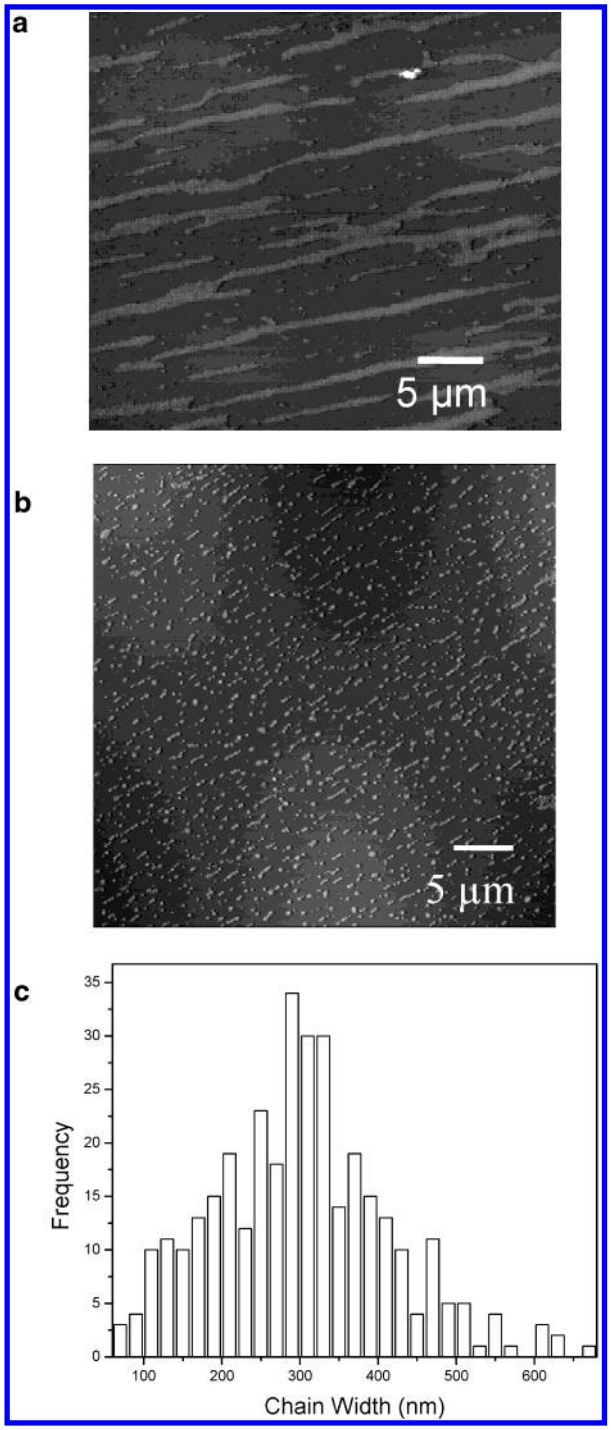

Figure 2. (a) AFM image of oriented particle chains at 0.8 T. (b) AFM image of oriented particle chains at 17 T. (c) Width distribution of the oriented chains. Majority have width of 300 nm.

an atomic force microscope. Figure 2a shows the pattern obtained at 0.8 T. At this field strength the particles are grouped into irregularly shaped, long (several microns in length), and narrow strands that are aligned with the field and joined at places. On the other hand, at the highest magnetic field of 17 T used in our study, which was obtained using an NMR spectrometer magnet, the strands had decomposed into discrete clusters (Figure 2b). At this field strength, the nanoparticles self-assemble into an ensemble of elongated clusters that are predominantly aligned lengthwise parallel to the applied field but have significant distribution of orientations about that direction. The clusters have a variety of shapes that exhibit a broad distribution in lengths, and a much narrower distribution in widths. In a statistical sampling of 340 clusters (in a 20 × 20 μm^2 area of an AFM image), the lengths of the clusters varied from 150 to 3500 nm, and the widths were narrowly grouped about 300 nm, which amounts to 25−30 particles across (Figure 2c). Magnetization measurements were performed on the system that was aligned with the 17 T field. These results are presented below.

The long-range self-assembly of magnetic nanoparticles is a complex process that involves numerous competing effects. These effects include the coupling of each particle's dipole moment to the applied field, magnetic dipole−dipole interactions, electronic polarization interactions (Helmholtz dipole layer and Van de Waals), and thermal kinetics, etc. Other factors influencing the self-assembly process include the properties of the media in which the particles are aligned, and the ambient conditions during alignment. Currently, there is no rigorous theory of this process that accounts for all of these effects and factors. Consequently, in this article, qualitative explanations of the experimental results are provided where possible.

In this experiment, self-assembly occurs at both the ensemble level (the distribution of cluster orientations), and at the cluster level (the orientation of nanoparticles within each cluster). At the ensemble level, the magnetization vector of each cluster couples to an effective field H_{eff} that is a superposition of the dominant applied field and a local "mean" field, which is due to the polarization and orientation of the neighboring clusters. To first order, an elongated cluster can be approximated as an ellipsoidal particle that has a shape-induced uniaxial anisotropy, with the easy axis along its length. The magnetostatic energy of the particle in the effective field is

$$E_s = \frac{1}{2}M^2N_cV + \frac{1}{2}(N_a - N_c)M^2V\sin^2(\theta) - H_{eff}MV\cos(\phi)$$

where N_a and N_c are the demagnetization factors along the a (short) and c (long) axes, respectively, θ is the angle between the magnetization vector and the easy axis, and ϕ is the angle between the effective field and the easy axis.[21] The energy will be a minimum when the cluster is aligned lengthwise with the effective field. However, the direction of the effective field can vary with respect to the applied field throughout the ensemble, because of the mean field contribution. This would account for the observed distribution of cluster orientations, which in turn, impacts the magnetic behavior of the ensemble.

The nanoparticles within each cluster have a uniaxial ansitropy and, therefore, tend to align with the applied field. However, their orientation will be influenced by dipole−dipole interactions with neighboring particles. The overall effect is that the particles will tend to orient in a head-to-tail (north-to-south) configuration with their easy axes aligned with the applied field, and with adjacent particles spatially staggered so as to minimize the local magnetostatic energy. Wiedwald et al. have observed a hexagonal network of particles in similar nanostructures.[22]

A superconducting quantum interference device (SQUID) was used to measure the magnetization of the sample. Hysteresis measurements were recorded with a static magnetic field applied first parallel, and then perpendicular to the direction of the array alignment. The applied field was systematically varied from −2000 to +2000 G. Two samples were studied. The first sample consisted of a two-dimensional array of nanoparticles on a GaAs substrate. No alignment field was applied during the self-assembly of this sample. The second sample consisted of a quasi one-dimensional array of nanoparticles and was subjected to an aligment field as described above. The first sample was measured at 300 K and exhibited superparamagnetic behavior

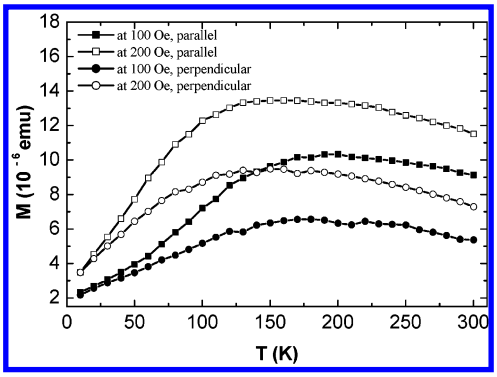

Figure 3. Blocking temperature from zero field cooled (ZFC) magnetization of oriented particles. Both have broad peaks about 170 K.

(Figure 4a). The second sample was measured at temperatures of 100 and 5K, which are well below the blocking temperature. The magnetization of the second sample was measured with zero-field-cooling (ZFC).

The magnetization curves of the second (aligned) sample obtained at 100 and 5K (below the blocking temperature) show a clear influence of the alignment field (Figure 4b,c). The coercive fields and the normalized remanence are significantly higher in the parallel versus perpendicular directions (Table 1). The coercivity values are slightly asymmetric with the left values somewhat larger than the right. This anomaly can be attributed to some measurement artifact possibly originating from the trap field in the SQUID magnet. Taking an average between the left and right values of coercivities, we find the coercivity along the parallel direction was ∼57% higher at 100 K, and this difference increased to approximately 136% at 5 K. Another point to note is the fact that the magnitude of magnetization in the perpendicular direction remains higher than that in the parallel direction. At present, we cannot provide any explanation for this behavior and it will be necessary to study if there is any tendency of the spins to be pinned in the perpendicular direction when sweeping the field, in the present configuration. Ideally, however, the saturation magnetization in either direction should be identical.

The higher coercivity and remanence along the parallel direction is due to the predominant alignment of the clusters in this direction. Specifically, a higher energy needs to be overcome to effect a reversal of magnetization in this direction. On the other hand, the reduced coercivity and remanence in the perpendicular direction can be explained by the distribution of cluster orientations. This can be understood from the anistropic behavior of a single particle with a uniaxial anisotropy. If the magnetization of such a particle is measured in a direction that is almost (but not exactly) perpendicular to the easy axis, a hysteresis curve is obtained that exhibits a much reduced coercivity and remanence relative to that obtained when the field is oriented along the easy axis (i.e., in the parallel direction).[21] In this experiment the distribution in cluster orientations can give rise to this effect because the applied field is never simultaneously perpendicular to the easy axis of all the clusters. Instead, it will be offset from this direction for a subset of clusters, and this will result in the observed reduced coercivity and remanence. Ngo et al., in a similar study of ferrite nanocrystals synthesized through microemulsion, found modest changes in the coercive fields between the two directions.[23]

The ZFC magnetization curves (Figure 3) show a strong directional dependence in the rise of magnetization with temperature (dM/dT), which was clearly larger for the parallel orientation. This is to be expected because alignment in the

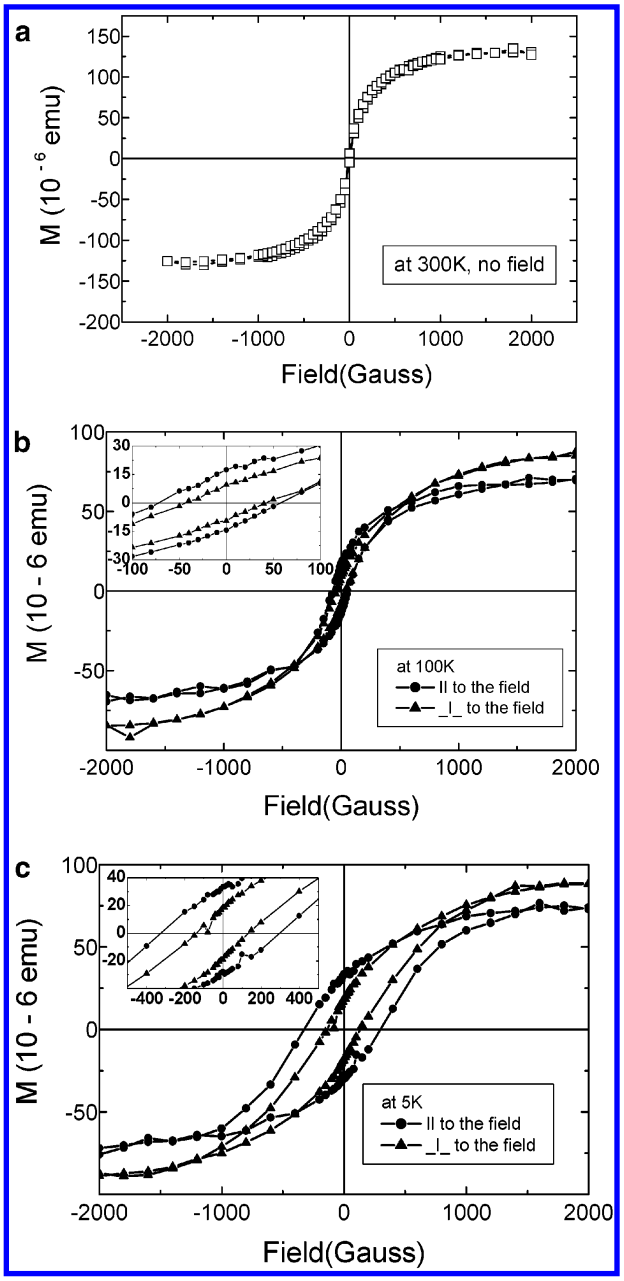

Figure 4. (a) Hysteresis loop of particles assembled with zero external field, measured at 300 K. (b) Hysteresis loop of oriented chains at 100 K. The coercivity difference is about 57%. (c) Hysteresis loop of oriented chains at 5 K. The coercivity difference is about 136%.

TABLE 1

T (K)	coercivity (G) parallel	coercivity (G) perpendicular	coercivity change (%)	M_r/M_{2000G} parallel	M_r/M_{2000G} perpendicular
5	315	133	136	0.454	0.250
100	64	42	57	0.279	0.103

parallel direction is more energetically favorable than in the perpendicular direction. It was difficult to determine a unique value of blocking temperatures, T_B, from the ZFC curves because of their relatively broad peaks. The broad peaks can be explained by the relatively broad distribution of observed cluster shapes. The distribution in shapes of the elongated clusters gives rise to a distribution of shape-induced anisotropy constants, which produce a distribution of blocking temperatures. The T_B in ZFC sensitively depends on the nanoparticles sizes, anisotroy and their interaction. In a recent publication, Kechrakos et al. observed an increase in the T_B, derived from ZFC of

a dense dispersion of ferromagnetic particles and attributed it to the anisotropic and ferromagnetic character of the dipolar interaction.[11] Also, Cui et al. have shown systematic changes in T_B with the variation in sizes.[24]

In summary, we have demonstrated a field-directed self-assembly of a system of magnetic nanoparticles on a substrate. The particles assemble into a distribution of elongated clusters, with a predominant orientation in the direction of the applied field. The system exhibits anisotropic hysteretic behavior below the blocking temperature T_B, with significantly higher coercivity and remanence parallel to the alignment field than perpendicular to it. ZFC magnetization curves show a similar directional dependence in the increase in magnetization with temperature (dM/dT) below T_B, and relatively broad peak regions. It is anticipated that field-directed self-assembly could be a viable alternative to lithography-mediated patterning for device purposes.

Acknowledgment. We acknowledge the help of X. Chen for magnetization measurement. This work was supported by a DURINT grant from the Chemistry and Life Sciences Directorate of the Air Force Office of Scientific Research through grant number F496200110358.

References and Notes

(1) Bean, C. P.; Livingstone, J. D. *J. Appl. Phys.* **1959**, *30*, 120S.
(2) Gunther, L., Barbara, B., Eds. *Quantum Tunneling of Magnetization*; Kluwer Academic Publishers: Dodrecht, The Netherlands, 1994.
(3) Poddar, P.; Fried, T.; Markovich, G. *Phys. Rev. B* **2002**, *65*, 172405.
(4) Black, C. T.; Murray, C. B.; Sandstrom, R. L.; Sun, S. *Science* **2000**, *290*, 1131.
(5) Speliotis, D. E. *J. Magn. Magn. Mater*. **1999**, *193*, 29.
(6) Raj, K.; Moskowitz, B.; Casciari, R. *J. Magn. Magn. Mater*. **1995**, *149*, 174.
(7) Ziolo, R. F.; Giannelis, E. P.; Weinstein, B. A.; O'Horo, M. P.; Ganguly, B. N.; Mehrotra, V.; Russell, M. W.; Huffman, D. R. *Science* **1992**, *257*, 219.
(8) Smyth, J. F.; Schultz, S.; Fredkin, D. R.; Kern, D. P.; Rishton, S. A.; Schmid, H.; Cali, M.; Koehler, T. R. *J. Appl. Phys*. **1991**, *69*, 5262.
(9) 9Hao, Y.; Castano, F. J.; Ross, C. A.; Vogeli, B.; Walsh, M.; Smith, H. I. *J. Appl. Phys*. **2002**, *91*, 7989.
(10) Held, G. A.; Grinstein, G.; Doyle, H.; Sun, S.; Murray, C. B. *Phys. Rev. B* **2001**, *64*, 012408.
(11) Kechrakos, D.; Trohidou, K. N. *Appl. Phys. Lett*. **2002**, *81*, 4574.
(12) Dormann, J. L.; Fiorani, D.; Tronc, E. *Adv. Chem. Phys*. **1997**, *98*, 283.
(13) Dormann, J. L.; Bessaiss, L.; Fiorani, D. *J. Phys. C* **1988**, *21*, 2015.
(14) Jonsson, T.; Svedlindh, P.; Hansen, M. F. *Phys. Rev. Lett*. **1998**, *81*, 3976.
(15) Papusoi, C., Jr. *J. Magn. Magn. Mater*. **1999**, *195*, 708.
(16) Luo, W.; Nagel, S. R.; Rosenbaum, T. F.; Rosensweig, R. E. *Phys. Rev. Lett*. **1991**, *67*, 2721.
(17) El-Hilo, M.; O'Grady, K.; Chantrell, R. W. *J. Magn. Magn. Mater*. **1992**, *114*, 307.
(18) Shtrikman, S.; Wohlfarth, E. P. *Phys. Lett. A* **1981**, *85* (8, 9) 467.
(19) Shtrikman, S.; Wohlfarth, E. P. *J. Magn. Magn. Mater*. **1983**, *31*−*34*, 1421.
(20) Massart, R. *IEEE Trans. Magn*. **1981**, *17*, 131.
(21) Morrish, A. H. *The Physical Principles of Magnetism*; Robert E. Kreiger Publishing Co.: Malabar, FL, 1983.
(22) Wiedwald, U.; Spasova, M.; Farle, M.; Hilgendorff, M.; Giersig, M. *J. Vac. Sci. Technol. A* **2001**, *19* (4), 1773.
(23) Ngo, A. T.; Pileni, M. P. *J. Phys. Chem. B* **2001**, **105**, 53; *J. Appl. Phys*. **2002**, *92*, 4649.
(24) Liu, C.; Zhang, Z. J. *Chem. Mater*. **2001**, *13*, 2092.